BIOCHEMISTRY
including biophysical chemistry & molecular biology
Article

Biochemistry **2009,** *48,* 7305–7312 7305
DOI: 10.1021/bi900175z

Site-Directed Mutagenesis as a Probe of the Acid−Base Catalytic Mechanism of Homoisocitrate Dehydrogenase from *Saccharomyces cerevisiae*[†]

Ying Lin, Ann H. West, and Paul F. Cook*

Department of Chemistry and Biochemistry, University of Oklahoma, 620 Parrington Oval, Norman, Oklahoma 73018

Received February 3, 2009; Revised Manuscript Received June 8, 2009

ABSTRACT: Homoisocitrate dehydrogenase (HIcDH) catalyzes the Mg^{2+}- and K^+-dependent oxidative decarboxylation of homoisocitrate to α-ketoadipate using NAD as the oxidant. A recent consideration of the structures of enzymes in the same family as HIcDH, including isopropylmalate and isocitrate dehydrogenases, suggests all of the family members utilize a Lys-Tyr pair to catalyze the acid−base chemistry of the reaction [Aktas, D. F., and Cook, P. F. (2009) *Biochemistry 48*, 3565−3577]. Multiple-sequence alignment indicates the active site Lys-Tyr pair consists of lysine 206 and tyrosine 150. Therefore, the K206M and Y150F mutants of HIcDH were prepared and characterized to test the potential roles of these residues as acid−base catalysts. The V/E_t values of the K206M and Y150F mutant enzymes at pH 7.5 are decreased by ∼2400- and ∼680-fold, respectively, compared to that of wild-type HIcDH; the K_m for HIc does not change significantly. V/E_t and $V/K_{MgHIc}E_t$ for the K206M mutant enzyme are pH-independent below pH 6 and decrease to a constant value above pH 7, while $V/K_{NAD}E_t$ is independent over the pH range from 6.2 to 9.5. In the case of the Y150F mutant enzyme, V/E_t and $V/K_{NAD}E_t$ are pH-independent above pH 9.5 and decrease to a constant value below pH 8. This behavior can be compared to that of the wild-type enzyme, where V/E_t decreases at high and low pH, giving pK_a values of ∼6.5 and ∼9.5, respectively. Data were interpreted in terms of a group with a pK_a of 6.5 that acts as a general base in the hydride transfer step and a group with a pK_a of 9.5 that acts as a general acid to protonate C3 in the tautomerization reaction [Lin, Y., Volkman, J., Nicholas, K. M., Yamamoto, T., Eguchi, T., Nimmo, S. L., West, A. H., and Cook, P. F. (2008) *Biochemistry 47*, 4169−4180]. Solvent deuterium isotope effects on V and V/K_{MgHIc} were near unity for the K206M mutant enzyme but ∼2.2 for the Y150F mutant enzyme. The dramatic decreases in activity, the measured solvent deuterium isotope effects, and changes in the pH dependence of kinetic parameters compared to that of the wild type are consistent with K206 acting as a general base in the hydride transfer step of the wild-type enzyme but as a general acid in the Y150F mutant enzyme, replacing Y150 in the tautomerization reaction. In addition, Y150 acts as a general acid in the tautomerization reaction of the wild-type enzyme and replaces K206 as the general base in the hydride transfer step of the K206M mutant enzyme.

Homoisocitrate dehydrogenase (3-carboxy-2-hydroxyadipate dehydrogenase, EC 1.1.1.87) (HIcDH)[1] catalyzes the conversion of homoisocitrate to α-ketoadipate (α-Ka) and CO_2 with NAD as the oxidant (*1*). The HIcDH is specific to the α-aminoadipate pathway (AAA) for lysine biosynthesis in fungi and higher plants and is a member of the family of pyridine nucleotide-dependent *β*-hydroxyacid oxidative decarboxylases (*2*). The reaction is metal ion-dependent, and the enzyme selectively binds the MgHIc chelate complex (*3*). A steady state random kinetic mechanism has been proposed for HIcDH; a preferred ordered release of CO_2, α-Ka, and NADH was proposed (*3*). The rate of the pathway with NAD being added prior to MgHIc is limited by a conformational change, presumably to close the active site prior to catalysis (*3*, *4*). Addition of MgHIc to enzyme followed by NAD gives a pathway with oxidative decarboxylation contributing to rate limitation. In addition, it was recently shown that the enzyme requires K^+ for optimum binding affinity for NAD at pH >7 (*4*). The role of the monovalent cation is likely to neutralize charge as a neutral acid in the dinucleotide binding site becomes unprotonated.

On the basis of the pH dependence of kinetic parameters and isotope effects, a general base−general acid chemical mechanism

[†]This work was supported by a grant from the Oklahoma Center for the Advancement of Science and Technology to P.F.C. (HR07-016), a grant (GM 071417) from the National Institutes of Health (to P.F.C. and A.H.W.), and the Grayce B. Kerr Endowment to the University of Oklahoma (to P.F.C.).

*Corresponding author: Email: pcook@ou.edu Tel: 405-325-4581 Fax: 405-325-7182.

[1]Abbreviations: HIcDH, homoisocitrate dehydrogenase; AAA, α-aminoadipate pathway; α-Ka, α-ketoadipate; NAD, nicotinamide adenine dinucleotide (the positive charge is omitted for convenience); NADH, reduced nicotinamide adenine dinucleotide; NADD, reduced nicotinamide adenine dinucleotide with deuterium in the 4-*R* position; TDH, tartrate dehydrogenase; Hepes, *N*-(2-hydroxyethyl)piperazine-*N*′-2-ethanesulfonic acid; Ches, 2-(*N*-cyclohexylamino)ethanesulfonic acid; Bis-Tris, bis(2-hydroxyethyl)iminotris(hydroxymethyl)methane; Tris, tris(hydroxymethyl)aminomethane; Ic, isocitrate; KAc, potassium acetate; TMAC, tetramethylammonium chloride; CMP, 3-carboxypropylidenemalate; MgHIc, chelate complex of magnesium and homoisocitrate; D_2O, deuterium oxide; DCl, deuterium chloride; NaOD, sodium deuterioxide; SKIE, solvent kinetic isotope effect; wt, wild-type HIcDH.

Published on Web 06/16/2009

Scheme 1: Proposed Chemical Mechanism of Homoisocitrate Dehydrogenase[a]

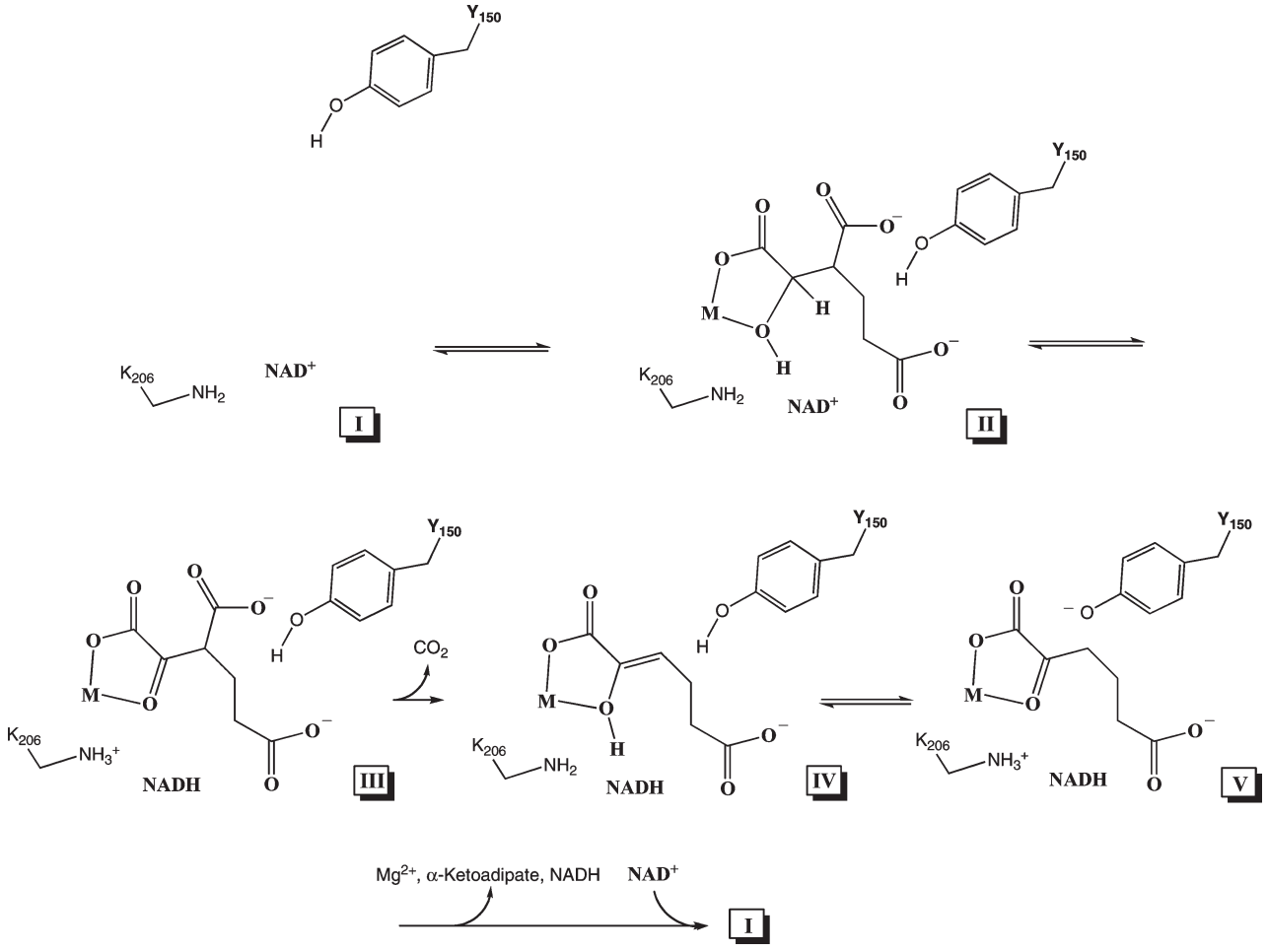

[a] The enzyme is in an open or partially open form upon binding of NAD (I) and closes upon binding of MgHIc, which brings Y150 into the proximity of HIc (II). Hydride transfer is facilitated by K206 acting as a base catalyst to generate 3-carboxy-α-ketoadipate (III). Decarboxylation occurs with the metal ion acting as a Lewis acid and K206 donating a proton to give the enol (IV). General base (K206)−general acid (Y150) catalysis then gives α-ketoadipate (V), and (I) is regenerated upon release of Mg^{2+} (M), α-ketoadipate, and NADH, and NAD binding. (The acid base chemistry could be catalyzed by K206 and Y150 directly or mediated by a water molecule for one residue or both residues.)

for HIcDH was proposed (Scheme 1) (*5*). A general base, with a pK_a of ~6.5, was proposed to accept a proton from the 2-hydroxyl of HIc as the 2-keto-3-carboxyadipate intermediate is formed in the hydride transfer step. The metal ion then acts as a Lewis acid and catalyzes the decarboxylation of the β-ketoacid, and the base, now acting as an acid, protonates the keto oxygen as the enol of α-ketoadipate is formed. Enol−keto tautomerization is then catalyzed by the base accepting a proton from the oxygen enol and a second enzyme group, with a pK_a of ~9.5, protonating C3 to give the final ketone product. The mechanism is very similar to those proposed for malic enzyme (*6*), isocitrate dehydrogenase (*7*, *8*), and tatrate dehydrogenase (*9*).

Although a structure of HIcDH is available, it is for the *Thermus thermophilus* enzyme and has no ligands bound to the active site (*10*). The structure of the bacterial HIcDH can be superimposed on those of the porcine IcDH (*11*) and bacterial IPMDH (*12*), which have ligands bound. Data suggest a conserved active site with a Lys-Tyr pair serving as general base and general acid catalysts. A review of the literature on the metal ion-dependent pyridine nucleotide-linked β-hydroxyacid oxidative decarboxylases has recently been written that suggests a very similar mechanism for this class of enzymes that makes use of very similar catalytic machinery (*13*). A multiple-sequence alignment of HIcDH with sequences of IcDH, IPMDH, and TDH suggests K206 and Y150 may function as the catalytic groups.

In this paper, site-directed mutagenesis was used to determine whether K206 and Y150 carry out the acid and base catalysis of HIcDH. Thus, K206 was changed to M, and Y150 was changed to F. The resulting mutant enzymes were characterized using initial rate studies and the pH dependence of kinetic parameters and isotope effects. Data are consistent with K206 serving as the catalytic base and Y150 as the general acid in the tautomerization step.

MATERIALS AND METHODS

Chemicals. Potassium acetate (KOAc) was obtained from Sigma. β-NAD and β-NADH were from USB. Hepes, Tris, Bis-Tris, and Ches buffers were from Research Organics, Inc. Deuterium oxide (D_2O) (99 atom % D) was purchased from Cambridge Isotope Labotories, Inc. α-Ketoadipate (*16*) and HIc (*3*) were prepared according to published procedures.

Enzymes. HIcDH was subjected to site-directed mutagenesis to generate the Y150F and K206M mutant enzymes. The plasmid

harboring the HIcDH gene was used as a template for mutagenesis, and the mutant enzymes were prepared using the QuikChange site-directed mutagenesis kit from Stratagene. Whole gene sequencing was performed for each of the mutations at the Laboratory for Genomics and Bioinformatics of the University of Oklahoma Health Science Center in Oklahoma City. The resulting sequence was compared to that of the wild-type HIcDH using BLAST. Successfully mutated plasmids were transformed into BL21(DE3) competent cells, the expression host. To engineer the Y150F mutant enzyme, the forward and reverse primers are CTGAGGACCTG**TTC**ATTAAAATTG and CAATTTTAAT**GAA**CAGGTCCTCAG, respectively, while for the K206M mutant enzyme, the forward and reverse primers are GACAGTGACTCAT**ATG**TCAAATGTTCTA TC and GATAGAACATTTGA**CAT**ATGAGTCACTGTC, respectively. The mutated codons are shown in bold.

Enzyme Assay. The activity of wt and mutant HIcDHs was measured using a Beckman DU 640 spectrophotometer to monitor the increase or decrease in absorbance at 340 nm as NAD is reduced to NADH. All assays were conducted at 25 °C. A unit of enzyme activity is defined as the amount of enzyme catalyzing the production or utilization of 1 μmol of NADH/min at 25 °C. Typical assays contained 100 mM buffer, 200 mM KOAc (saturating for both mutant enzymes), 4.2 μM MgHIc, and 0.5 mM NAD in a 1 mL volume. The final concentration of HIcDH in the cuvette was 15 nM for the wild-type enzyme and ~1 μM for the mutant enzymes. In the case of the mutant enzymes, the total concentration of HIc (HIc plus MgHIc) was at least 10 times greater than the concentration of MgHIc; i.e., HIc was 10 times MgHIc. Thus, the lowest ratio of HIc_{total} to enzyme is 10 for any of the assays carried out.

pH Studies. The pH dependence of V and V/K for all substrates was measured under conditions in which one substrate concentration was varied with the other maintained at saturation ($\geq 10K_m$). The pH was maintained using the following buffers at 100 mM: Bis-Tris for pH 5.0−6.8, Hepes for pH 6.8−8.2, and Ches for pH 8.2−10.0. Hepes and Ches were titrated to the appropriate pH with KOH, while Bis-Tris was titrated using HCl. Sufficient overlap was obtained upon changing buffers to detect buffer effects; none were observed. The ionic strength of the reaction mixtures over the pH range of our measurements is approximately constant at 0.1. The pH was recorded before and after initial velocity data were measured with observed changes limited to ≤0.1 pH unit. The enzymes were stable when incubated for at least 15 min over the pH range of 5.0−10.0. pH−rate profiles were initially evaluated graphically by plotting log V or log(V/K) versus pH to determine the proper equation for data fitting and to assess the quality of data.

Solvent Deuterium and Viscosity Effects. Initial velocities were measured in H_2O and D_2O. For rates measured in D_2O, substrates and buffers were first dissolved in a small amount of D_2O and lyophilized overnight to remove exchangeable protons. The lyophilized powders were then dissolved in D_2O to give the desired concentration, and the pD was adjusted using NaOD. A value of 0.4 was added to the pH meter reading to calculate pD (*17*). Data were obtained by varying one substrate at a fixed concentration ($10K_m$) of the other. The isotope effects were obtained by direct comparison of initial rates in H_2O and D_2O at pH(D) 8.0. Reactions were initiated by adding 5 μL of enzyme solution in H_2O, such that the final percentage of D_2O was ~99%. The concentration of the enzyme stock solution was adjusted depending on the specific activity.

Initial velocities were determined in H_2O at a relative viscosity of 1.24 at pH 8.0 and 25 °C; assays contained 9% glycerol (w/v) as the viscosogen, which generates the same relative viscosity as 100% D_2O at 25 °C (*18*). A standard curve (relative viscosity vs glycerol) was constructed to determine the amount of glycerol needed for a relative viscosity of 1.24 (*19*).

Circular Dichroism (CD) Spectra. CD spectra were recorded on an Aviv 62DS spectropolarimeter at 25 °C with a path length of 0.2 cm. Enzyme concentrations of 100 μg/mL were used for far-UV CD spectra. The buffer used for all spectra was 10 mM phosphate (pH 7.0), and a buffer blank was subtracted from each spectrum. Spectra were collected with a dwell time of 3 s and were the average of three spectra. Far-UV spectra were measured from 200 to 250 nm.

Data Analysis. Initial velocity data were first analyzed graphically using double-reciprocal plots of initial velocities versus substrate concentration and suitable secondary plots. Data were then fitted using the appropriate equation, and the Marquardt−Levenberg algorithm supplied with the EnzFitter program from BIOSOFT (Cambridge, U.K.). Kinetic parameters and their corresponding standard errors were estimated using a simple weighting method.

Data obtained as a function of MgHIc concentration at different fixed levels of NAD were fitted using eq 1. Data for solvent deuterium isotope effects on V and V/K were fitted using eq 2.

$$v = \frac{VAB}{K_{ia}K_b + K_aB + K_bA + AB} \quad (1)$$

$$v = \frac{VA}{K_a(1+F_iE_{V/K}) + A(1+F_iE_V)} \quad (2)$$

In eqs 1 and 2, v and V are initial and maximum velocities, respectively, A and B are substrate concentrations, K_a and K_b are Michaelis constants for substrates A and B, respectively. In eq 1, K_{ia} is the dissociation constant for the EA complex. In eq 2, F_i is the fraction of D_2O in the solvent and $E_{V/K}$ and E_V are the solvent deuterium isotope effects minus 1 on V/K and V, respectively.

Data for pH−rate profiles with a limiting slope of 1 at low pH were fitted using eq 3, while data for pH−rate profiles that exhibit a partial change at low or high pH were fitted using eq 4 or 5.

$$\log y = \log\left[C/\left(1+\frac{H}{K_1}\right)\right] \quad (3)$$

$$\log y = \log\left[\frac{Y_L + Y_H\left(\frac{H}{K_2}\right)}{1+\frac{H}{K_2}}\right];\ \log y - \log\left[\frac{Y_L + Y_H\left(\frac{H}{10^{-6}}\right)}{1+\frac{H}{10^{-6}}}\right] \quad (4)$$

$$\log y = \log\left[\frac{Y_L + Y_H\left(\frac{K_2}{H}\right)}{1+\frac{K_2}{H}}\right] \quad (5)$$

In eq 3, y is the observed value of V/K_{MgHIc} for the K206M mutant enzyme at any pH, C is the pH-independent value of y, H is the hydrogen ion concentration, and K_1 is the acid dissociation constant for an enzyme or substrate functional group that

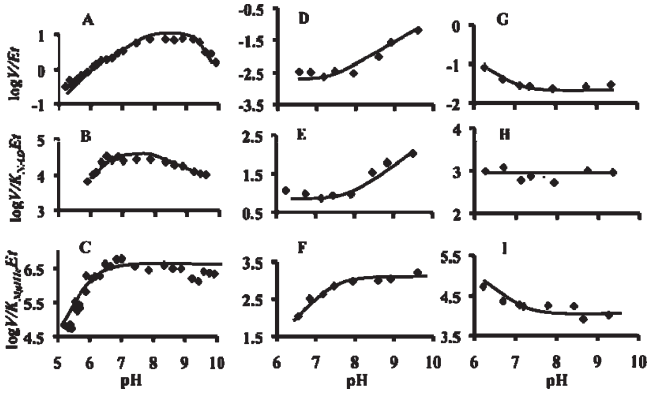

FIGURE 1: pH dependence of kinetic parameters for wild-type and mutant enzymes. Data for wt (A−C) are from ref *5*. (D−F) K206M mutant enzyme. (G−I) Y150F mutant enzyme. Units for V/E_t and V/KE_t are s^{-1} and M^{-1} s^{-1}, respectively. All data were obtained at 25 °C. Points are the experimentally determined values. The curves are theoretical and based on fits to eq 5 for panels D and E, eq 3 for panel F, and eq 4 for panels G and I. The average value is shown for $V/K_{NAD}E_t$. Error bars are included in the size of the data point.

must be unprotonated for optimal binding and/or catalysis. In eqs 4 and 5, y is the observed value of V or V/K and Y_L and Y_H are the pH-independent values of y at low and high pH, respectively. In eq 4, K_2 is the acid dissociation constant for enzyme or substrate functional groups that must be unprotonated for optimal binding and/or catalysis, while in eq 5, the group must be protonated for optimal binding and/or catalysis. V/E_t and $V/K_{MgHIc}E_t$ for the Y150F mutant enzyme decrease from a constant value at low pH to a lower constant value at high pH. Attempts to fit the data to eq 4 were unsuccessful. The observed pH dependence (Figure 1) indicates a pK_a of ≤6, and a group with a pK_a of ~6.5 is observed for the wt enzyme (*5*). Thus, K_2 in eq 4 was fixed at 10^{-6} M, and data were fitted to generate estimates of Y_L and Y_H.

RESULTS

Expression and Purification of Mutant Enzymes. Expression and purification of the Y150F and K206M mutant enzymes were very similar to those of wt (*3*). The purity of the wild-type and mutant enzymes was >95% on the basis of SDS−PAGE. Far-UV CD spectra were very similar for the mutant and wt enzymes, suggesting the overall structure of the mutant enzymes is intact and changes are likely restricted to the active site.

Kinetic Parameters of the Y150F and K206M Mutant Enzymes. Initial rates were measured at pH 7.5 as a function of NAD at different fixed concentrations of MgHIc for both mutant enzymes. Double-reciprocal plots intersected to the left of the ordinate, consistent with the sequential kinetic mechanism reported previously (*3*). Kinetic parameters are summarized in Table 1, compared to those obtained for wt.

Replacing Y150 with F or K206 with M results in a decrease of 680- or 2400-fold, respectively, in V/E_t. K_{MgHIc} is not greatly affected for either of the mutant enzymes, giving decreases in $V/K_{MgHIc}E_t$ that reflect the change in V/E_t. Although K_{NAD} is increased by only ~2-fold in the case of the K206M mutant enzyme, it is decreased 10-fold for the Y150F mutant enzyme. As a result, the value of $V/K_{NAD}E_t$ is decreased by only 70-fold in the case of the Y150F mutant enzyme.

Rescue of Activity by Small Molecules. Addition of small molecules can, in some cases, rescue activity lost when important functional groups are eliminated from an enzyme side chain. Replacement of Y150 with F results in the elimination of a hydroxyl group, and it is unlikely that addition of small molecules would have an effect. Addition of 10 mM NH_4Cl or $(NH_4)_2SO_4$ had no effect. However, in the case of K206M, addition of the same components resulted in a 30% increase in V/E_t.

pH−Rate Profiles. The pH dependence of kinetic parameters obtained previously for the wild-type enzyme is reproduced in Figure 1 for comparison to those of the mutant enzymes (*5*). V/E_t gives estimated pK_a values of ~7.1 and ~9.5. A hollow is observed in the curve as the pH decreases, i.e., the curve exhibits a plateau at pH ~6.5, before it eventually decreases with a limiting slope of 1. $V/K_{NAD}E_t$ decreases at low pH, giving a pK_a value of ~6.4, while a partial change is observed at high pH, giving a pK_a value of ~8.3. $V/K_{MgHIc}E_t$ decreases at low pH with a limiting slope of +2, with an average pK_a value of ~6.0. One of the groups observed in the $V/K_{MgHIc}E_t$ pH−rate profile likely reflects the substrate, which has a pK_a for its third ionization of 5.8 (*5*).

The pH dependence of kinetic parameters for the K206M mutant enzyme differs considerably from those of wt and the Y150F mutant enzymes (Figure 1D−F). The V/E_t pH−rate profile is pH-independent at pH >9.5 and decreases to a lower constant value below a pK_a of 9.6 ± 0.2. The pH-independent values of V/E_t at high and low pH are 0.13 ± 0.02 and 0.002 ± 0.001 s^{-1}, respectively (1 and 0.015% of the V/E_t of wt, respectively). The $V/K_{NAD}E_t$ pH−rate profile is similar to that of V/E_t and exhibits a pK_a of 9.0 ± 0.1, and pH-independent values at high and low pH are 140 ± 8 and 9.0 ± 0.1 M^{-1} s^{-1}, respectively (0.5 and 0.03% of the values of wt, respectively). However, $V/K_{MgHIc}E_t$ is pH-independent above pH 7.5 and exhibits the requirement for a group that must be unprotonated for optimal activity and/or binding. The observed pK_a is 7.3 ± 0.1, and the pH-independent value of $V/K_{MgHIc}E_t$ is 1120 ± 40 M^{-1} s^{-1} (0.04% of the value of wt).

The V/E_t for the Y150F mutant enzyme decreases from a constant value below pH 6 to a lower constant value at high pH (Figure 1G−I). As discussed in Data Analysis, a pK_a of 6.0 was assumed to allow estimates of the low- and high-pH constant values; the value at low pH is 0.110 ± 0.002 s^{-1}, while that at high pH is 0.026 ± 0.002 s^{-1} (0.8 and 0.2% of the V/E_t of wt, respectively). The pH dependence of $V/K_{MgHIc}E_t$ is similar to that of V/E_t, and data were fitted as for V/E_t with an assumed pK_a of 6.0. pH-independent values of ~(1.28 ± 0.06) × 10^5 and ~(1.0 ± 0.1) × 10^4 M^{-1} s^{-1} are estimated at low and high pH, respectively (4 and 3% of the values of wt, respectively). On the other hand, $V/K_{NAD}E_t$ is pH-independent and exhibits an average value of ~903 ± 9 M^{-1} s^{-1} (3% of the value of wt). Quantitative anaylsis (see Discussion) of the data will make use of the estimated pH-independent values presented above.

Dependence of Kinetic Parameters on Solvent Deuterium and Solvent Viscosity. Finite solvent deuterium isotope effects of ~1.2 and ~2.4 are observed on V and V/K_{MgHIc} for Y150F, while equal values of ~2.2 are observed for the two parameters for K206M (Table 2). The wt enzyme exhibits a finite SKIE on V, but an inverse effect on V/K_{MgHIc} that was attributed to the increase in viscosity resulting from 100% D_2O. As a result, the effect of 9% glycerol, which gives a viscosity equal to 100% D_2O (1.24) on the kinetic parameters of the mutant enzymes, was determined. As seen in Table 2, the K206M mutant enzyme exhibits no effect of increased viscosity. The Y150F mutant enzyme, on the other hand, exhibits significant deceases in V and

Table 1: Kinetic Parameters for Wild-Type and Mutant Enzymes at pH 7.5

	wild type	Y150F	K260M
V/E_t (s^{-1})	13 ± 1	0.019 ± 0.001	0.0054 ± 0.0005
x-fold decrease	1	680 ± 60	2400 ± 290
$V/K_{NAD}E_t$ (M^{-1} s^{-1})	(2.9 ± 0.6) × 10^4	(4.2 ± 0.4) × 10^2	6.0 ± 0.6
x-fold decrease	1	70 ± 16	4800 ± 1100
$V/K_{MgHIc}E_t$ (M^{-1} s^{-1})	(3.1 ± 0.7) × 10^6	(1.8 ± 0.1) × 10^3	(1.8 ± 0.6) × 10^3
x-fold decrease	1	1700 ± 400	1700 ± 700
K_{NAD} (mM)	0.45 ± 0.08	0.045 ± 0.004	0.84 ± 0.02
x-fold change	1	10 ± 2 (decrease)	1.9 ± 0.3 (increase)
K_{MgHIc} (μM)	4.2 ± 0.9	1.06 ± 0.02	3 ± 1
x-fold decrease	1	4.0 ± 0.9	1.4 ± 0.6

Table 2: Effects of Solvent Deuterium and Solvent Viscosity on the HIcDH Mutant Enzymes

				H_2O/D_2O		H_2O/9% glycerol in H_2O	
enzyme	fixed substrate	varied substrate	pH	$D_2O(V)$	$D_2O(V/K)$	$^n(V)$	$^n(V/K)$
wt[a]	NAD ($10K_m$)	MgHIc	8.0	2.5 ± 0.2	1.3 ± 0.2	1.5 ± 0.2	0.6 ± 0.1
wt[a]	NAD ($10K_m$)	Ic	8.0	0.94 ± 0.08	0.69 ± 0.08	0.66 ± 0.03	0.6 ± 0.1
Y150F	NAD (5 mM)	MgHIc	8.0	1.24 ± 0.06 (0.97 ± 0.06)	2.4 ± 0.3 (1.3 ± 0.1)	1.28 ± 0.06	1.8 ± 0.2
K206M	NAD (15 mM)	MgHIc	8.0	2.3 ± 0.4	2.1 ± 0.7	1.0 ± 0.1	1.0 ± 0.2

[a] From ref *5*.

V/K_{MgHIc} (Table 2). Correction of the SKIE for the viscosity effect gives residual effects of ~1 and ~1.3 on V and V/K_{MgHIc}.

DISCUSSION

Kinetic Mechanism. The large decreases in V/E_t observed for the Y150F (500-fold; high pH-independent value) and K206M (6500-fold; low pH-independent value) mutant enzymes are consistent with the importance of these residues in the catalytic mechanism. Changes in the K_m values for reactants are minimal, with the exception of K_{NAD} for the Y150F mutant enzyme, which is decreased by ~10-fold. As a result, $V/K_{NAD}E_t$ is decreased by a factor of only 70, while in all other cases, the decrease in V/K reflects the decrease in V.

The initial rate of the wild-type enzyme reaction is limited by a conformational change triggered by the binding of MgHIc (*3*). The structural change is likely required to generate the catalytic conformation prior to catalysis (see Correlation of Kinetic and Structural Data). The primary deuterium isotope effect obtained by direct comparison of initial rates with NADH(D) is within error unity, indicating the net rate constant for the chemical steps is ≥10-fold faster than the rate constant for the conformational change.[2] Changing Y150 to F and K206 to M likely affects the chemical steps in the oxidative decarboxylation reaction (see the introductory section). Thus, the decrease in the net rate constant of the chemical step must be underestimated. In the case of the Y150F mutant enzyme, the decrease must be ≥5000-fold [$10(V/E_t)_{wt}/(V/E_t)_{Y150F} = 5000$], while that for the K206M mutant enzyme must be ≥65000-fold [$10(V/E_t)_{wt}/(V/E_t)_{K206M} = 65000$]. The approximately 5 × 10^3- to 6.5 × 10^4-fold decreases observed for the two mutant enzymes are consistent with their proposed function as acid−base catalysts. The dramatic decrease in the rate constant of the chemical step(s) of the mutant enzymes compared to those of wt indicates the kinetic mechanism will be rapid equilibrium and not steady state. Initial velocity patterns obtained by measuring the initial rate as a function of NAD at different fixed levels of MgHIc (data not shown) are consistent with a random mechanism.[3]

Isotope Effects. As suggested above, K206 and Y150 likely serve as the general base and general acid, respectively, in the oxidative decarboxylation reaction. Primary deuterium isotope effects were measured for wt by direct comparison of initial rates with NADH(D) as the labeled reactant. In the case of the mutant enzymes, the effect could not be measured because of the very low rate in the direction of reductive carboxylation (*3*). However, solvent deuterium kinetic isotope effects were measured (Table 2). The wild-type enzyme exhibits a normal solvent isotope effect on V and V/K_{MgHIc} once corrected for solvent viscosity effects. On the basis of primary kinetic deuterium and ^{13}C isotope effects and multiple primary deuterium/solvent deuterium and solvent deuterium/^{13}C effects, data were interpreted in terms of a rate-limiting conformational change prior to the chemical steps with MgHIc limiting, and additionally a contribution to rate limitation by the tautomerization step with substrates saturating. An inverse solvent kinetic deuterium isotope effect was associated with the conformational change prior to catalysis (*5*).

The K206M mutant enzyme exhibited a normal isotope effect of ~2.2 on V and V/K_{MgHIc}. The wt enzyme exhibited a finite viscosity effect with the relative viscosity of the medium fixed at that of D_2O, 1.24. No viscosity effect was observed for the K206M mutant enzyme. The normal solvent isotope effect is almost certainly a result of the transfer of a proton from the

[2] The intrinsic isotope effect on the hydride transfer step is likely > 3, the estimated value of ^Dk in the 6-phosphogluconate dehydrogenase reaction (*14*); the estimated value of the effect in the malic enzyme reaction is ~10 (*15*). Given a value of 3 for ^Dk, and the general equation for the deuterium isotope effect [$^D(V/K) = (^Dk + k_{chem}/k_{conf})/(1 + k_{chem}/k_{conf})$], a value of 10 for k_{chem}/k_{conf} would almost completely suppress the isotope effect. If the value of ^Dk is 10, the value of k_{chem}/k_{conf} would have to be > 100.

[3] The K_m for the first substrate bound in a rapid equilibrium ordered kinetic mechanism is zero. This results from the ability of high concentrations of B to trap A in central complexes, as long as the concentration of A is slightly greater than the concentration of enzyme.

2-hydroxyl of HIc as it is oxidized to α-keto-3-carboxyadipate in the hydride transfer step. The hydride transfer step is likely rate-determining for the mutant enzyme (see pH−Rate Studies), as expected for an enzyme without its general base. The normal solvent kinetic deuterium isotope effect is in agreement with a lack of contribution to rate limitation from the conformational change prior to catalysis.

The Y150F mutant enzyme exhibits very little if any solvent deuterium kinetic isotope effect, once corrected for the significant effect of viscosity (Table 2). The ketonization of the enol of α-ketoadipate is likely the slow step along the reaction pathway of the Y150F mutant, given the absence of the tyrosine hydroxyl, which is believed to serve as the general acid that protonates C3 of the enol. The low value of the solvent isotope effect suggests that if the tautomerization is slow, there must be either an early or late transition state for the proton transfer. Since water likely takes the place of the tyrosine hydroxyl in the ketonization reaction of Y150F, and water is not a good base, the transition state is more likely to be late for the proton transfer. As for the normal K206M mutant enzyme, the solvent kinetic deuterium isotope effect is not inverse, consistent with rate limitation by steps(s) other than the conformational change prior to catalysis.

Interpretation of pH−Rate Profiles. Homoisocitrate dehydrogenase from *Saccharomyces cerevisiae* exhibits a steady state random kinetic mechanism; the predominant pathway is that with addition of MgHIc prior to NAD (*3*). The dominant species present when V/K_{MgHIc} and V/K_{NAD} are measured are E-NAD and MgHIc, and E:MgHIc and NAD, respectively. The pH dependence under these conditions will reflect a group(s) on the reactant and/or enzyme that is important for binding and/or catalysis. The pH dependence of V will reflect a group(s) on the enzyme that is important for catalysis (*20*).

A general acid−general base mechanism has been previously proposed for wt on the basis of the pH−rate profiles shown in Figure 1 and isotope effects (*5*). On the basis of the dramatic decreases in the values of kinetic parameters of the K206M and Y150F mutant enzymes, the slight rescue of K206M by ammonia, and structural data (see Correlation of Kinetic and Structural Data), data are interpreted in terms of an acid−base mechanism with K206 as the base and Y150 as the acid. For wt, a mechanism was proposed in which a general base with a pK_a of 6.5−7 acts to accept the proton from the 2-hydroxyl of HIc (or Ic) and a general acid with a pK_a of ∼9.5 acts to protonate C3 once decarboxylation has occurred. The pK_a of 9.5 is only observed in the V pH−rate profile with MgHIc as a substrate, suggesting the tautomerization of the enol of adipic acid contributed to rate limitation at saturating reactant concentrations (*5*). The V/E_t pH−rate profiles for the mutant enzymes exhibit pK_a values that are very similar to those observed for wt, 6 for the Y150F mutant enzyme and 9.5 for the K206M mutant enzyme. However, the pH dependencies are opposite those of wt, with the Y150F enzyme exhibiting the requirement for a group with a pK_a of ∼6 that must be protonated for maximum activity and the K206M enzyme exhibiting the requirement for a group with a pK_a of 9.5 that must be unprotonated for maximum activity.

The V/E_t and $V/K_{NAD}E_t$ values of the K206M mutant enzyme decrease below pH 10, giving a pK_a value of 9.3, to a lower constant value below pH 8. Overall, this represents an increase by >2 pH units in the intrinsic pK_a of 6.5−7 for the base of wt (*5*). Of interest, the pK_a is within error identical to that observed on the basic side of the V/E_t pH−rate profile for wt using HIc as the substrate. The latter pK_a was attributed to the general acid that protonates the enol of α-ketoadipate in the tautomerization reaction. The pH-independent value of V/E_t obtained with the group unprotonated is ∼0.1 s^{-1}, 90-fold lower than that of wt. It is likely that the group, Y150, that functions as the general acid in the wt enzyme now serves as a base, either directly or mediated via a water molecule, to accept a proton from the α-hydroxyl of HIc in the overall reaction in the absence of K206. With Y150 acting optimally as a base, at pH values above 9.5, the 90-fold lower value of V/E_t compared to that of wt indicates a single base is not sufficient for the overall reaction. Formally, the reaction requires transfer of a proton from the α-hydroxyl of HIc to C3 of α-ketoadipate, which could be catalyzed by a single group. However, the geometry of the proton transfer reactions is likely not easily satisfied. The similarity in pH behavior of V/E_t and $V/K_{NAD}E_t$ suggests the same steps limit the reaction with NAD limiting and with all reactants saturating. On the other hand, $V/K_{MgHIc}E_t$ decreases at low pH, giving a pK_a of ∼7.4. This group is not observed in the pH−rate profile for V, suggesting the presence of a group that must be unprotonated for optimal binding of MgHIc. The group is not observed in the pH−rate profiles for the wt or Y150F mutant enzyme. It is thus unmasked once K206 has been eliminated. The identity of the group will have to await further studies.

The pH-independent value of V/E_t for K206M at pH <8 is ∼0.002 s^{-1}, which is 6500-fold lower than the value of V/E_t obtained for wt, and 65-fold lower than the pH-independent value at pH <6 of the K206M mutant enzyme (0.13 s^{-1}). At pH 7.5, a SKIE of ∼2.3 is measured, suggesting hydride transfer is rate-limiting, as suggested above. The $\Delta\Delta G^{\ddagger}$ estimated from the ratio of $(V/E_t)_{wt}/(V/E_t)_{K206M}$ is 5.3 kcal/mol, which provides a lower limit to the contribution of K206 to base catalysis. The value of 0.002 s^{-1} is still greater than the value for the uncatalyzed reaction, which would be extremely low for this multistep reaction and is an indicator that the remaining catalytic functionalities in the active site, not the least of which is the metal ion, together perhaps with active site water, contribute significantly to catalysis.

The V/E_t value of the Y150F mutant enzyme decreases at pH >6 [a pK_a value of about 6 was assumed (see Materials and Methods)] to a lower constant value at pH >7. The general shape of the $V/K_{MgHIc}E_t$ pH−rate profile is very similar to that of V/E_t, while the $V/K_{NAD}E_t$ pH−rate profile is pH-independent. The general base, presumably K206, now acts as a general acid, taking the place of Y150 in the tautomerization reaction. The pK_a of the base decreases from ∼6.5−7 in wt to ∼6 in Y150F. Thus, elimination of Y150 results in a decrease in the pK_a, likely as a result of a more hydrophilic environment around the lysine. The pH independence of $V/K_{NAD}E_t$ suggests the positive charge on the nicotinamide ring of NAD also affects the pK_a of K206. The pH-independent value of V/E_t obtained with the group protonated in Y150F is ≥0.11 s^{-1}, similar to that of the K206M mutant enzyme with Y150 protonated. It is likely that, in the Y150 mutant enzyme, K206 functions as the general acid and protonates C3 of the enol of α-ketoadipate. With K206 acting optimally as an acid, at pH <6, the ≥90-fold lower value of V/E_t compared to that of wt indicates a single group is not sufficient for the overall reaction, as is true for K206M.

The pH-independent value of V/E_t for Y150F above pH 7 is 0.026 s^{-1}, which is 500-fold lower than the value of V/E_t obtained for wt, and 4-fold lower than the low pH-independent value (0.11 s^{-1}) of the Y150F mutant enzyme. Over this pH range, the SKIE is ∼1, indicating a proton is not in flight in the rate-limiting

transition state. The $\Delta\Delta G^{\ddagger}$ estimated from the ratio of $(V/E_t)_{wt}/(V/E_t)_{Y150F}$ is 3.7 kcal/mol, which provides a lower limit to the contribution of Y150 to base catalysis.[4] The value of 0.026 s^{-1} is still greater than the value for the uncatalyzed reaction, which would be extremely low for this multistep reaction, and is an indicator that the remaining catalytic functionalities in the active site contribute significantly to catalysis as suggested for K206M.

Another possible explanation of the pH dependence of kinetic parameters of the mutant enzymes is the direct use of H_3O^+ and OH^- in Y150F and K206M, respectively. This is a possibility in the case of the Y150F mutant enzyme but is unlikely for the K206M mutant enzyme. V/E_t and $V/K_{NAD}E_t$ clearly approach a limiting value above pH 9 and give a fitted pK_a of ~9, very similar to the V/E_t value observed for wt (*5*). Data suggest the use of Y150 as a general base in the K206M-catalyzed reaction, as discussed above. It is thus likely that K206 serves as an acid in the Y150F mutant enzyme. However, even if H_3O^+ and OH^- are used directly, data are consistent with the acid−base catalytic properties of K206 and Y150 in the HIcDH reaction.

Correlation of Kinetic and Structural Data. A recent review of the enzymes in the class of pyridine nucleotide β-hydroxyacid oxidative decarboxylases suggests, on the basis of structure, that all of the enzymes in the class utilize the same catalytic machinery, i.e., a Lys-Tyr pair, to catalyze the reaction. The subclass of enzymes that catalyze the oxidative decarboxylation of (*R*)-β-hydroxyacids is dimeric, and the active site is comprised of residues from both subunits (*13*). The structure of the HIcDH from *T. thermophilus* (*10*) superimposes on the other members of the subclass quite well (*13*). The structure of HIcDH, prior to binding substrates is in an open form, shows Y150 is distant from the active site lysine (K206); Y150 is contributed by the other subunit in the dimer. However, a conformational change is required to close the site upon substrate binding, and this results in Y150 being in the proximity of homoisocitrate (*10*).

Data obtained in these studies are consistent with the proposed acid−base catalytic role of K206 and Y150 in the mechanism of HIcDH (Scheme 1). The open form of the enzyme is shown prior to binding MgHIc with Y150 away from the substrate-binding pocket (I). Binding of MgHIc gives the Michaelis complex with catalytic and binding groups in the proper orientation for the hydride transfer step (II). In this complex, K206 and Y150 are neutral; the neutral form of K206 is likely a result of the overall positive nature of the active site (*13*). Hydride transfer from C3 of HIc to the nicotinamide ring of NAD results in the 3-carboxy-α-ketoadipate intermediate (III). Decarboxylation occurs with the metal ion (M) acting as a Lewis acid and K206 donating a proton to give the enol of α-ketoadipate (IV). Tautomerization to generate the final ketone product makes use of K206 acting as a base to accept the enol proton and Y150 acting to protonate C3 (V). Release of products and binding reactants then completes the catalytic cycle; this also requires an intramolecular transfer of a proton from K206 to Y150, presumably mediated by solvent.

Elimination of K206 results in a low pH-independent level of activity, which increases as the pH increases above 8 and Y150 becomes unprotonated and can act as a base in the hydride transfer step (II in Scheme 1), which is almost certainly rate-determining for K206M. A water molecule bridging the C2 hydroxyl of HIc and Y150 may be required in this step. On the other hand, the Y150F mutant enzyme exhibits behavior that is the mirror image with a low pH-independent activity at high pH that increases as the pH decreases below 7. Data suggest the ability of K206 to act as an acid catalyst, donating a proton to form the enol (IV in Scheme 1). As in the case of K206M, this step may be mediated by a water molecule that bridges C2 of α-ketoadipate and K206. There are other conserved residues in the active site, but none appear to be properly positioned to carry out acid−base catalysis. However, the structure available is an apoenzyme, and additional structural and mechanistic work is required to test the proposed mechanism.

[4]As suggested in footnote 2, the values are likely at least an order of magnitude lower than those estimated from the observed values. This would give a value of ≥6.6 kcal/mol for K206 and ≥5.1 kcal/mol for Y150.

ACKNOWLEDGMENT

We thank Rong Guan for preparing panels D−I of Figure 1. We thank Tadashi Eguchi from the Tokyo Institute of Technology for the 3-carboxypropylidenemalate.

REFERENCES

1. Strassman, M., and Ceci, L. N. (1965) Enzymatic Formation of α-Ketoadipic Acid from Homoisocitric Acid. *J. Biol. Chem. 240*, 4357–4361.
2. Karsten, W. E., and Cook, P. F. (2000) Pyridine Nucleotide-Dependent β-Hydroxyacid Oxidative Decarboxylases: An Overview. *Protein Pept. Lett. 7*, 281–286.
3. Lin, Y., Alguindigue, S. S., Volkman, J., Nicholas, K. M., West, A. H., and Cook, P. F. (2007) Complete Kinetic Mechanism of Homoisocitrate Dehydrogenase from *Saccharomyces cerevisiae*. *Biochemistry 46*, 890–898.
4. Lin, Y., West, A. H., and Cook, P. F. (2008) Potassium Activates Homoisocitrate Dehydrogenase by Increasing the Affinity for NAD. *Biochemistry 47*, 10809–10815.
5. Lin, Y., Volkman, J., Nicholas, K. M., Yamamoto, T., Eguchi, T., Nimmo, S. L., West, A. H., and Cook, P. F. (2008) Chemical Mechanism of Homoisocitrate Dehydrogenase from *Saccharomyces cerevisiae*. *Biochemistry 47*, 4169–4180.
6. Karsten, W. E., Liu, D. L., Rao, G. S. J., Harris, B. G., and Cook, P. F. (2005) A Catalytic Triad is Responsible for Acid-Base Chemistry in the *Ascaris suum* NAD-Malic Enzyme. *Biochemistry 44*, 3626–3635.
7. Kim, T. K., Lee, P., and Colman, R. F. (2003) Critical Role of Lys (212) and Tyr(140) in Porcine NADP-dependent Isocitrate Dehydrogenase. *J. Biol. Chem. 278*, 49323–49331.
8. Lee, P., and Colman, R. F. (2006) Thr(373), Asp(375), and Lys(260) Are in the Coenzyme Site of Porcine NADP-dependent Isocitrate Dehydrogenase. *Arch. Biochem. Biophys. 450*, 183–190.
9. Karsten, W. E., Tipton, P. A., and Cook, P. F. (2002) Tartrate Dehydrogenase Catalyzes a Stepwise Oxidative Decarboxylation of D-Malate with NAD^+ or thioNAD^+ as the Dinucleotide Substrate. *Biochemistry 41*, 12193–12199.
10. Miyazaki, J., Asada, K., Fushinobu, S., Kuzuyama, T., and Nishiyama, M. (2005) Crystal Structure of Tetrameric Homoisocitrate Dehydrogenase from an Extreme Thermophile, *Thermus thermophilus*: Involvement of Hydrophobic Dimer-Dimer Interaction in Extremely High Thermotolerance. *J. Bacteriol. 187*, 6779–6788.
11. Ceccarelli, C., Grodsky, N. B., Ariyaratne, N., Colman, R. F., and Bahnson, B. J. (2002) Crystal Structure of Porcine Mitochondrial $NADP^+$-dependent Isocitrate Dehydrogenase Complexed with Mn^{2+} and Isocitrate: Insights Into the Enzyme Mechanism. *J. Biol. Chem. 277*, 43454–43462.
12. Imada, K., Inagaki, K., Matsunami, H., Kawaguchi, H., Tanaka, H., Tanaka, N., and Namba, K. (1998) Structure of 3-Isopropylmalate Dehydrogenase in Complex with 3-Isopropylmalate at 2.0 Å Resolution: The Role of Glu88 in the Unique Substrate Recognition Mechanism. *Struct. Folding Des. 6*, 971–982.
13. Aktas, D. F., and Cook, P. F. (2009) A Lysine-Tyrosine Pair Carries Out Acid-Base Chemistry in the Metal Ion-Dependent Pyridine Dinucleotide-Linked β-Hydroxyacid Oxidative Decarboxylases. *Biochemistry 48*, 3565–3577.
14. Li, L., Dworkowski, F. S. N., and Cook, P. F. (2006) Import of the 6-Phosphate of in the Binding of 6-Phosphogluconate in the 6-Phosphogluconate Dehydrogenase Reaction. *J. Biol. Chem. 281*, 25568–25576.

15. Karsten, W. E., and Cook, P. F. (1994) Stepwise versus Concerted Oxidative Decarboxylation Catalyzed by Malic Enzyme: A Reinvestigation. *Biochemistry 33*, 2096–2103.
16. Nelson, R. B., and Gribble, G. W. (1973) On the Preparation of α-Ketoadipic Acid. *Org. Prep. Proced. Int. 5*, 55–58.
17. Schowen, K. B., and Schowen, R. L. (1982) Solvent Isotope Effects on Enzyme Systems. *Methods Enzymol. 87*, 551–606.
18. Quinn, D. M., and Sutton, L. D. (1991) in Enzyme Mechanism from Isotope Effects (Cook, P. F., Ed.) pp 73−126, CRC Press, Boca Raton, FL.
19. Bazelyansky, M., Robey, E., and Kirsch, J. F. (1986) Fractional Diffusion-limited Component of Reactions Catalyzed by Acetylcholinesterase. *Biochemistry 25*, 125–130.
20. Cook, P. F., and Cleland, W. W. (2007) Enzyme Kinetics and Mechanism , Garland Press, London.